

# SIESTA: Efficient Online Continual Learning with Sleep

Md Yousuf Harun<sup>1\*</sup> Jhair Gallardo<sup>1\*</sup> Tyler L. Hayes<sup>1†</sup>

Ronald Kemker<sup>2</sup> Christopher Kanan<sup>3</sup>

Rochester Institute of Technology<sup>1</sup>, United States Space Force<sup>2</sup>, University of Rochester<sup>3</sup>

## Abstract

In supervised continual learning, a deep neural network (DNN) is updated with an ever-growing data stream. Unlike the offline setting where data is shuffled, we cannot make any distributional assumptions about the data stream. Ideally, only one pass through the dataset is needed for computational efficiency. However, existing methods are inadequate and make many assumptions that cannot be made for real-world applications, while simultaneously failing to improve computational efficiency. In this paper, we do not propose a novel method. Instead, we present SIESTA, an incremental improvement to the continual learning algorithm REMIND. Unlike REMIND, SIESTA uses a wake/sleep framework for training, which is well aligned to the needs of on-device learning. SIESTA is far more computationally efficient than existing methods, enabling continual learning on ImageNet-1K in under 3 hours on a single GPU; moreover, in the augmentation-free setting it matches the performance of the offline learner, a milestone critical to driving adoption of continual learning in real-world applications.

## 1. Introduction

Training DNNs is incredibly resource intensive. This is true for both learning in highly resource constrained settings, e.g., on-device learning, and for training large production-level DNNs that can require weeks of expensive cloud compute. Moreover, for real-world applications, the amount of training data typically grows over time. This is often tackled by periodically re-training these production systems from scratch, which requires ever-growing computational resources as the dataset increases in size. Continual learning algorithms have the ability to learn from ever-growing data streams, and they have been argued as a potential solution for efficient learning for both embedded and large production-level DNN systems, improving the computational efficiency of network training and updating [52]. However, continual learning is rarely used for real-world

\*Equal contribution.

†Now at NAVER LABS Europe.

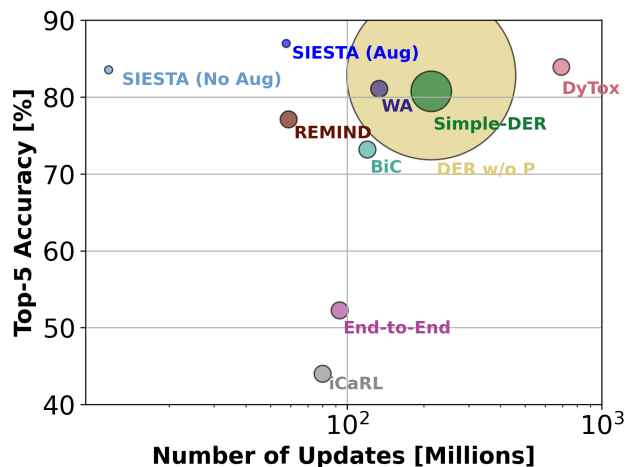


Figure 1: Our method, SIESTA, outperforms existing continual learning methods for class-incremental learning on ImageNet-1K while requiring fewer network updates and using fewer parameters, as denoted by circle size.

applications because these algorithms fail to achieve comparable performance to offline retraining or they make assumptions that do not match real-world applications. In this paper, we describe a resource efficient, continual learning algorithm that rivals an offline learner on supervised tasks, a critical milestone toward enabling the use of continual learning for real-world applications.

In conventional offline training of DNNs, training data is shuffled (making it independent and identically distributed (iid), which is required for stochastic gradient descent (SGD) optimization) and repeatedly looped through many training iterations. In contrast, an ideal continual learning algorithm is able to efficiently learn from *potentially* non-iid data streams, where each training sample is only seen by the learner once unless a limited amount of auxiliary storage is used to cache it. Most continual learning algorithms are designed solely to overcome catastrophic forgetting, which occurs when training with non-iid data [52, 39]. To do this, most models make implicit or explicit assumptions that go beyond the general supervised learning setting, e.g., some

methods assume the availability of additional information or assume a specific structure of the data stream. Moreover, existing methods do not match the performance of an offline learner, which is essential for industry to adopt continual learning for updating large DNNs.

We argue that a continual learning algorithm should have the following properties:

1. It should be capable of online learning and inference in a compute and memory constrained environment,
2. It should rival (or exceed) an offline learner, regardless of the structure of the training data stream,
3. It should be significantly more computationally efficient than training from scratch, and
4. It should make no additional assumptions that constrain the supervised learning task, e.g., using task labels during inference.

These criteria are simple; however, most continual learning algorithms make strong assumptions that do not match real-world systems and are assessed on toy problems that are not appropriate surrogates for real-world problems where continual learning could greatly improve computational efficiency. For example, many works still focus on tasks such as split-CIFAR100 [57, 78, 17, 74, 18], only work in extreme edge cases like incremental class learning [9, 11, 32, 58, 67, 73], assume the availability of task-labels during inference [24, 21, 34, 62], or require large batches to learn [74, 18]. For continual learning to have practical utility, we need efficiency and performance that rivals trained from scratch models, as well as robustness to data ordering.

There are two extreme frameworks for continual learning. At one extreme, is incremental batch learning where the agent receives a batch and has as much time as necessary to loop over that batch before proceeding to the next batch. Typically these systems are evaluated with large batches, and many experience dramatic performance decreases when smaller batches are used [26]. At the other extreme is online continual learning, where the agent receives one input at a time. Humans and animals learn in a manner that is a compromise between these two extremes. They acquire new experiences in an online manner and these experiences are consolidated offline during sleep [49, 29]. Sleep plays a role in memory consolidation in all animals studied, including invertebrates, birds, and mammals [70]. While animals sleep to consolidate memories, they can use both consolidated (post-sleep) and recent (pre-sleep) experiences to make inferences while awake.

Although this paradigm is virtually ubiquitous among animals, it has rarely been studied as a paradigm in continual learning. This paradigm matches a real-world need: on-device continual learning and inference. For example, virtual/augmented reality (VR/AR) headsets could use continual learning to establish play boundaries and to identify locations in the physical world to augment with virtual over-

lays. Home robots, smart appliances, and smart phones need to learn about the environments and the preferences of their owners. In all of these examples, learning online is needed, but there are large periods of time where offline memory consolidation is possible, e.g., while the mobile device is being charged or its owner is asleep. In this paper, we formalize this paradigm for continual learning and we describe an algorithm with these capabilities, which we call SIESTA (Sleep Integration for Episodic STreAming).

SIESTA is a variant of REMIND [26] that is designed to operate in our online learning with offline consolidation paradigm. REMIND continually trains the upper layers of a deep neural network (DNN) in a pseudo-online manner. It stores quantized mid-level representations of seen inputs in a buffer, which enables it to store a much larger number of samples with a given memory budget compared to methods that store raw images. To do pseudo-online training, REMIND uses rehearsal [30], a method for mitigating catastrophic forgetting by mixing new inputs with old inputs. For every new input, REMIND reconstructs a small number of past inputs, mixes the new input with them, and updates the DNN with this mini-batch; however, using rehearsal for every sample to be learned is not ideal. SIESTA addresses this by using rehearsal only during its offline sleep stage. For online learning, SIESTA instead uses lightweight online updates of the DNN’s output layer.

#### Our major contributions are summarized as:

1. We formalize a framework for online learning with offline memory consolidation, and we describe the SIESTA algorithm that operates in this framework (see Fig. 2). SIESTA is capable of rapid online learning and inference while awake, but has periods of sleep where it performs offline memory consolidation.
2. For incremental class learning on ImageNet-1K, SIESTA achieves state-of-the-art performance using far fewer parameters, memory, and computational resources than other methods. Without augmentations, training SIESTA requires only 2.4 hours on a single NVIDIA A5000 GPU. In contrast, recent methods require orders of magnitude more compute (see Fig. 1).
3. SIESTA is the first continual learning algorithm to achieve identical performance to an offline model, when augmentations are not used. It solves *catastrophic forgetting* - the most studied problem in continual learning (see Table 1). SIESTA is capable of working with arbitrary orderings, and achieves similar performance in both class incremental and iid settings.

## 2. Online Learning with Offline Consolidation

We formalize the classification problem setting for supervised online continual learning with offline consolidation. The learner alternates between an online phase and an offline phase. For learning, during the  $j$ 'th online phase, the agent receives a sequence of  $n$  labeled observations, i.e.,  $t_{j1}, t_{j2}, \dots, t_{jn}$ , where each input observation  $x_t$  has label  $y_t$ . The sequence is not assumed to be stationary, and it can contain examples from classes from an arbitrary label ordering. The agent can cache these labeled pairs, or a subset of them, in memory with storage of size  $b$  bits. The agent can be evaluated at any time during the online phase, where it must make inferences using both recent experiences from the  $j$ 'th online phase, as well as past experiences from previous phases. During the subsequent offline consolidation phase, the agent is allowed at most  $m$  updates of the network, e.g., gradient descent updates. We do not assume task labels are available during any phase. In general, iid (shuffled) orderings do not cause catastrophic forgetting; and at the other extreme, an ordering sorted by category causes severe catastrophic forgetting in conventional algorithms [39].

With some exceptions [38, 54, 55, 5], this paradigm has been little studied and offers several advantages. For example, it allows embedded mobile devices to quickly use new information from users and their environments and then consolidate that learning during a scheduled downtime. It also serves as a setting for studying learning efficiency in continual learning, where different sleep policies can be studied for minimizing the number of updates  $m$  during a sleep setting. Lastly, it allows for testing functional hypotheses from neuroscience about sleep. While rehearsal-like mechanisms used in continual learning occur during slow wave sleep, the mechanisms that occur during rapid eye movement (REM) sleep have not yet been explored with DNNs nor has the interplay between slow wave sleep and REM sleep. REM sleep increases abstraction, facilitates pruning of synapses, and is when dreams occur [63, 16, 7, 42, 20, 43]. We juxtapose our training paradigm with alternatives in continual learning in Sec. 3.

## 3. Related Work

We compare SIESTA's online learning with offline consolidation paradigm to alternative paradigms.

**Task Incremental Learning with Task Labels.** Incremental task batch learners [40, 77, 3, 10, 11, 62, 15], learn from task batches, where each batch has a distinct task that is often a binary classification problem. These methods assume the task label is available during evaluation so that the correct "output" head can be selected, and when this assumption is violated these methods fail [27, 26]. SIESTA

does not require task labels for prediction, which are typically not available in real-world applications.

**Incremental Class Batch Learning.** In this paradigm, a dataset is split into multiple batches, where each batch consists of mutually exclusive categories, without any revisiting of categories. An agent is given a batch to learn for as long as it likes and typically can use some auxiliary memory for rehearsal. This paradigm has been studied with rehearsal-based methods [29, 1, 6, 9, 11, 22, 25, 26, 32, 58, 67, 73] that store previously observed data in a memory buffer or reconstruct them to rehearse alongside new data. It has also been studied in regularization based methods [11, 3, 10, 15, 40, 21, 13, 44, 48, 59, 62, 77] that constrain new weight updates to penalize large deviations from past weights, as well as dynamic methods [18, 19, 75, 31, 51, 61, 74] that incrementally increase the capacity of a DNN over time. While task labels are not used during prediction, evaluation takes place between batches and many methods require large batches (e.g., thousands of examples) or they fail [26]. Some methods use a large number of parameters for keeping copies of the network in memory for distillation [9, 37]. In contrast, SIESTA can perform inference at any time and can operate in scenarios where classes are revisited.

**Online Continual Learning.** Unlike batch learning paradigms, in online continual learning, an agent observes data sequentially and learns them instance-by-instance in a single pass through the dataset. To study catastrophic forgetting, examples are typically ordered by class, although alternative orders are sometimes studied [26]. Evaluation can occur at any point during training. This setting eliminates looping over data many times and evaluation between batches, thus making it more efficient in terms of memory and compute time, which is desirable for embedded devices. This paradigm has primarily been studied on smaller datasets (CIFAR-100) [48, 11, 4, 71], although some methods have been shown to scale to ImageNet-1K [27, 25, 27, 23]. For ImageNet-1K, these methods under-perform incremental batch learning methods. SIESTA's paradigm is a compromise that captures most of the benefits of online continual learning, while enabling increased accuracy.

**Paradigm Relationships.** The formal online continual learning with offline consolidation setting can be configured to mirror other continual learning settings. For incremental class batch learning, where the learner receives large batches of training examples (e.g.,  $n > 100,000$  for ImageNet-1K [58, 74]), buffer  $b = b_{\text{recent}} + b_{\text{buffer}} + b_{\text{auxiliary}}$  would be sufficiently large to hold all  $n$  observations from the  $j$ 'th online phase ( $b_{\text{recent}}$ ) as well as past examples used for rehearsal ( $b_{\text{buffer}}$ ), and any additional memory needed for

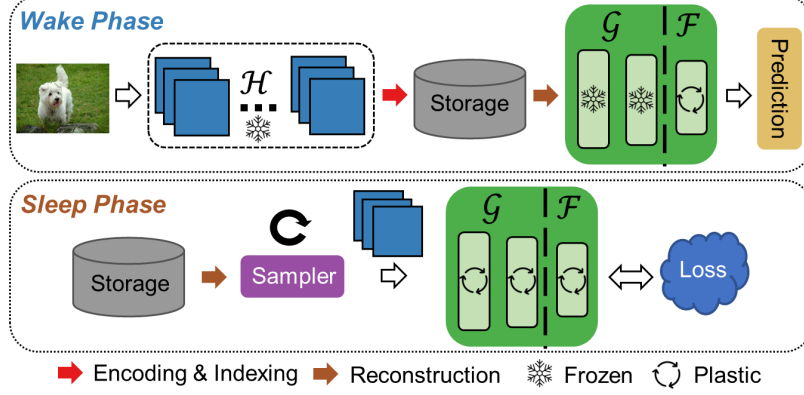


Figure 2: A high-level overview of SIESTA. During the *Wake Phase*, it transforms raw inputs into intermediate feature representations using network  $\mathcal{H}$ . The inputs are then compressed with tensor quantization and cached. Then, weights belonging to recently seen classes in network  $\mathcal{F}$  are updated with a running class mean using the output vectors from  $\mathcal{G}$ . Finally, inference is performed on the current sample. During the *Sleep Phase*, a sampler uses a rehearsal policy to choose which examples should be reconstructed from the cached data for each mini-batch. Then, networks  $\mathcal{G}$  and  $\mathcal{F}$  are updated with backpropagation in a supervised manner. The wake/sleep cycles alternate.

other purposes ( $b_{\text{auxiliary}}$ ) (e.g., distillation), and  $m$  is typically very large (e.g., for the state-of-the-art DyTox method,  $m > 500n$  [18]). A pseudo-online algorithm like REMIND [26] uses a configuration of  $n = 1$  and  $m = 51$ . For both REMIND and SIESTA,  $b$  only acts as a buffer for storing compressed past observations and their labels.

#### 4. The SIESTA Algorithm

The SIESTA algorithm (Fig. 2) alternates between awake and sleep phases. The awake phase involves online learning as well as sample compression, storage, and inference. The sleep phase involves memory consolidation via brief periods of offline learning. SIESTA is designed to handle data streams with arbitrary class orders, ranging from iid to class incremental paradigms.

SIESTA is a feed-forward DNN defined as  $\mathcal{F}(\mathcal{G}(\mathcal{H}(\cdot)))$ , where  $\mathcal{H}(\cdot)$  contains the bottom layers,  $\mathcal{G}(\cdot)$  contains the top layers prior to the output layer, and  $\mathcal{F}(\cdot)$  is the output layer. Specifically, SIESTA takes as input a 3rd-order tensor  $\mathbf{X}$ .  $\mathcal{H}(\cdot)$  produces  $\mathbf{Z} = \mathcal{H}(\mathbf{X})$ , where  $\mathbf{Z} \in \mathbb{R}^{r \times s \times d}$ ,  $r$  and  $s$  are the tensor spatial dimensions, and  $d$  are the tensor channel dimensions. This tensor is then transformed into a vector embedding, i.e.,  $\mathbf{z} = \mathcal{G}(\mathbf{Z})$ . The output layer  $\mathcal{F}(\cdot)$  is then described with cosine softmax, where the score for the  $k$ 'th class is given by:

$$p_k = \frac{\exp(a_k \tau^{-1})}{\sum_j \exp(a_j \tau^{-1})}, \quad (1)$$

where

$$a_k = \frac{\mathbf{f}_k^T \mathbf{z}}{\|\mathbf{f}_k\|_2 \|\mathbf{z}\|_2}, \quad (2)$$

$\mathbf{f}_k$  is the weight vector for the  $k$ 'th class, and  $\tau \in \mathbb{R}$  is a learned temperature used during optimization. It has been proven that cosine softmax encourages greater class separation than softmax [41]. In our implementation,  $\mathcal{H}$  and  $\mathcal{G}$  are both convolutional networks; however, other architectural choices would be suitable.

Following [26], prior to continual learning, the DNN is initialized by pre-training on an initial set of  $N$  training samples, e.g., images from the first 100 classes of ImageNet. Tensor features  $\mathbf{Z}$  are extracted from each of the  $N$  samples and used to fit a Product Quantization (PQ) model [35] to all  $rsN$   $d$ -dimensional vectors in these tensors. This enables us to efficiently store and reconstruct compressed representations of  $\mathbf{Z}$ . This approach enables SIESTA to much more efficiently use memory for rehearsal than methods that store raw images. The network  $\mathcal{H}(\cdot)$  is then kept fixed during continual learning. While this aspect of SIESTA is the same as REMIND, SIESTA differs significantly in its capabilities and how it is trained. REMIND uses replay during online learning, but SIESTA does not require replay during its online phase. Additionally, SIESTA performs offline learning phases periodically, while REMIND does not. We next describe how the online and offline learning phases operate.

##### 4.1. Online Learning while Awake

During the awake phase (see Fig. 2), only the output layer  $\mathcal{F}$  of the DNN is updated. This enables SIESTA to avoid catastrophic forgetting and permits lightweight online updates. When SIESTA receives an input tensor  $\mathbf{X}_t$  at time  $t$ ,  $\mathbf{Z}_t$  is then compressed and saved in a limited-sized stor-



age buffer using PQ along with its class label. If the buffer is full, then a randomly selected sample is removed from the class with the most samples. Subsequently, the output layer weights are updated with simple running updates for the appropriate class. The update for the output layer weight vector for class  $k$  is given by

$$\mathbf{f}_k \leftarrow \frac{c_k \mathbf{f}_k + \mathbf{z}_t}{c_k + 1}, \quad (3)$$

where  $c_k$  is an integer counter for class  $k$ . After updating the weight vector,  $c_k$  is incremented, i.e.,  $c_k \leftarrow c_k + 1$ . For inference, the class with the highest score  $p_k$  in Eq. 1 is selected as the predicted class.

## 4.2. Memory Consolidation During Sleep

During the sleep phase (see Fig. 2), the output layer  $\mathcal{F}$  and the top layers  $\mathcal{G}$  are trained using rehearsal, while the bottom layers  $\mathcal{H}$  are kept frozen. Rehearsal consists of selecting mini-batches of stored examples in the buffer for reconstruction and then using them to update the network with backpropagation. Following the paradigm in Sec. 2, the DNN is allowed at most  $m$  gradient descent updates. Given a mini-batch of size  $q$ , each sleep cycle therefore consists of updating the DNN with  $n$  mini-batches, where the total number of updates is  $m = q \times n$ . At the beginning of a sleep cycle, the samples chosen for reconstruction are governed by a policy. We compare multiple policies for selecting the samples to reconstruct in Sec. S3, but our main results all use balanced uniform sampling, i.e., sampling an equal number from each class, which worked best on class balanced datasets and was competitive on long-tailed ones.

While augmentation is typically applied directly to images, here we apply it to the reconstructed  $\mathbf{Z}$  tensors. We use two forms of augmentation: manifold mix-up [69] and cut-mix [76]. Both strategies are used in the standard manner, except instead of producing a weighted combination of two images, we create a weighted combination of tensors.

In our main results, we have the network sleep every  $120K$  samples, which in the incremental class learning setting corresponds to training on 100 categories. We study the impact of sleep frequency in Sec. 6.2.

## 4.3. Network Architecture & Initialization

While continual learning is starting to use transformers [18], recent work has primarily used ResNet18 [58, 73, 9, 73, 26, 74]. However, ResNet18 has been shown to perform worse than other similarly sized DNNs [28]. Moreover, given one of the major applications of continual learning is on-device learning, using a DNN designed for embedded devices is ideal. Therefore, in our main results, we use MobileNetV3-L [33]. MobileNetV3-L is lightweight with  $2 \times$  fewer parameters than ResNet18 and has lower latency.

Table 1: Experimental results on ImageNet-1K. For a fair comparison, we constrain methods to 12.5 million updates and do not use data augmentation. The ( $\uparrow$ ) and ( $\downarrow$ ) indicate high and low values to reflect optimum performance respectively.  $\mathcal{P}$  is the number of parameters in Millions,  $\mu$  is the average top-5 accuracy,  $\alpha$  is the final top-5 accuracy,  $\mathcal{M}$  is the total memory in GB, and  $\mathcal{U}$  is the total number of updates in Millions.

Method	$\mathcal{P}(\downarrow)$	$\mu(\uparrow)$	$\alpha(\uparrow)$	$\mathcal{M}(\downarrow)$	$\mathcal{U}(\downarrow)$
Offline	5.48	—	83.31	192.87	768.70
DER	54.80	81.87	70.15	20.99	12.43
REMIND	5.48	81.77	74.31	2.02	11.53
<b>SIESTA</b>	<b>5.48</b>	<b>88.33</b>	<b>83.59</b>	<b>2.02</b>	<b>11.53</b>

Since PQ encodes features across channels, MobileNetV3-L is more suitable for compressing its features with relatively less reconstruction error than ResNet18. We compare MobileNetV3-L and ResNet18 in Sec. S4.

During pre-training (i.e., base initialization), we adopt the approach used in [23], where the entire network is pre-trained using the self-supervised learning algorithm SwAV [8]. In [8], SwAV worked significantly better than supervised pre-training, as the features transferred more effectively to classes unseen during pre-training. We also use SwAV with DER [74] and REMIND [26].

Using MobileNetV3-L, we set network  $\mathcal{H}$  to be the first 8 layers of the network, consisting of 2.19% of the network parameters. Using images of size  $224 \times 224$  pixels,  $\mathcal{H}$  produces a tensor  $\mathbf{Z} \in \mathbb{R}^{14 \times 14 \times 80}$ . For PQ, we use *Optimized Product Quantization (OPQ)* from FAISS [36], which is used to compress and reconstruct the  $14^2$  80-dimensional vectors that make up each tensor. Following REMIND, we exclusively use reconstructed versions of the output of  $\mathcal{H}$  during continual learning. The remaining 11 layers of MobileNetV3-L, consisting of 97.81% of the network parameters, are trained during continual learning. An additional study of the quantization layer for MobileNetV3-L is in Sec. S5.

## 5. Experimental Setup

**Comparison Models.** We compare SIESTA to a variety of baseline and state-of-the-art methods, including online learners REMIND [26], SLDA [27], NCM [50]; incremental batch learners iCaRL [58], BiC [73], End-to-End [9], WA [78], Simple-DER [45], DER [74], DyTox [18]; and an offline learner. We compare with two variants of DER: DER without pruning (referred to as DER $\dagger$ ) and DER with pruning (referred to as DER $\ast$ ). These methods have been designed to be effective for incremental class learning on ImageNet-1K, and more details are in Sec. S1. SIESTA is trained with cross-entropy loss and uses SGD as its opti-

mizer with the OneCycle learning rate (LR) scheduler [64] during each sleep phase. It uses a higher initial LR in the last layer to help learn the new tasks and a lower LR in earlier layers to mitigate forgetting of previously learned information. For each sleep cycle, we use a batch size of 64, momentum 0.9, weight decay  $1e-5$ , an initial LR of 0.2 for the last layer, and an initial LR of 0.07 for the earlier layers. Additional details of SIESTA and implementation details for other methods are provided in Sec. S2.

**Datasets and Evaluation Criteria.** For our main results, we use ImageNet ILSVRC-2012, which is the standard object recognition benchmark for testing a model’s ability to scale [60]. It has 1.2 million images uniformly distributed across 1000 categories. We also use a long-tailed version of Places to evaluate rehearsal policies (see Sec. S3 for details). We configure the datasets in the continual iid setting and the class incremental learning setting, where data is ordered by class and images are shuffled within each class.

For evaluation, we report the average accuracy  $\mu$  over all steps  $T$ , where  $\mu = \frac{1}{T} \sum_{t=1}^T \alpha_t$ , with  $\alpha_t$  referring to the accuracy at step  $t$ . We also report the final accuracy  $\alpha$ . We use top-5 accuracy for ImageNet-1K and top-1 accuracy for Places. Additionally, we measure the total number of parameters  $\mathcal{P}$  (in millions) and the total memory  $\mathcal{M}$  (in gigabytes) used by each model. We also measure the total number of updates  $\mathcal{U}$ , where an update consists of a backward pass on a single input.

## 6. Results

### 6.1. Comparison with the Offline Learner

We first compare SIESTA, DER, and REMIND to an offline learner. For many real-world applications, a continual learner that performs significantly worse than an offline learner is unacceptable. Moreover, for these applications we cannot make assumptions about the data stream’s class order distribution; so for SIESTA and REMIND, we study both the class incremental and iid continual learning settings, which can be seen as an extreme best case and extreme worst case scenarios. DER, as designed, is only capable of incremental class learning. SIESTA, DER, and REMIND use the same SwAV pre-trained MobileNetV3-L DNN on the first 100 classes of ImageNet-1K. The offline learner is a MobileNetV3-L trained from scratch.

We first show results where all models do not use augmentations, including the offline learner. SIESTA used 1.28M updates per sleep cycle. All continual learners used a similar total number of updates. Results for incremental class learning are given in Table 1 and learning curves in Fig. 3. Both DER and REMIND perform over 9% worse (absolute) than the offline learner for final accuracy. SIESTA had similar final accuracy for both the class incre-

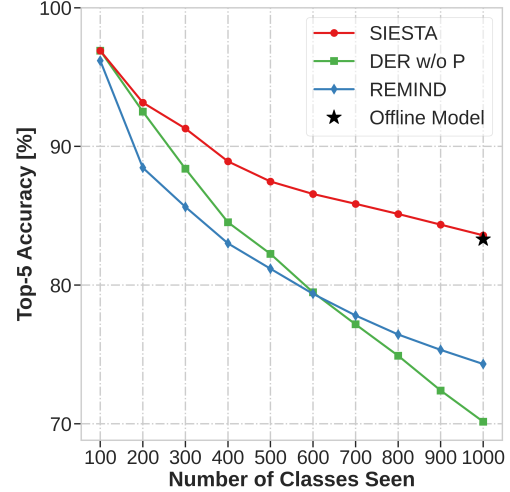


Figure 3: ImageNet-1K learning curves without data augmentation during training.

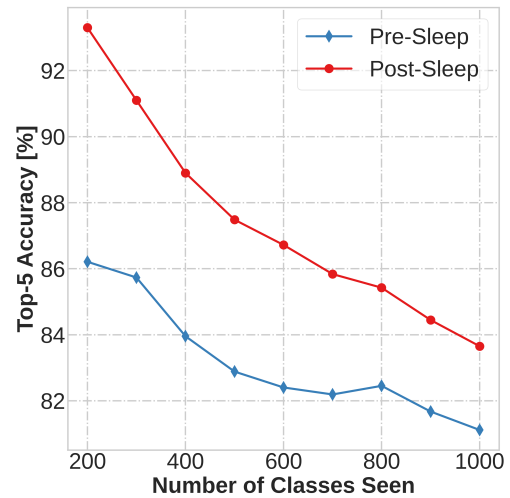


Figure 4: Learning curves of SIESTA’s pre- and post-sleep performance as a function of seen classes.

mental (83.59%) and iid (83.45%) scenarios, whereas REMIND performed better in the iid setting (79.52%) than the class incremental setting (74.31%). Using Cochran’s Q test [12], a non-parametric paired statistical test that can be used for comparing multiple classifiers, we found there was no significant difference among SIESTA’s final accuracy for the iid and class incremental settings compared to the offline learner ( $P = 0.08$ ). Therefore, SIESTA achieves “no forgetting” by matching the performance of the offline MobileNetV3-L across orderings. We conducted a similar analysis when augmentations are used in Sec. S6.

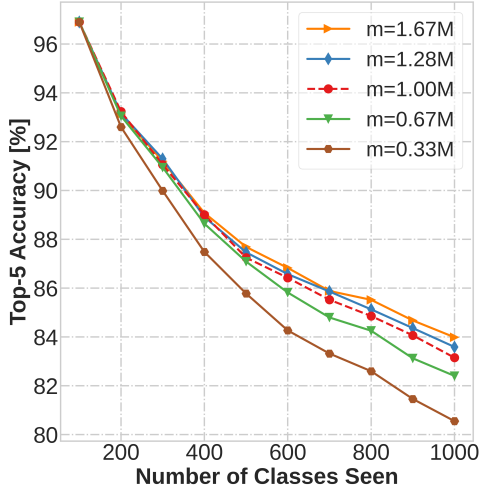


Figure 5: The impact of sleep length  $m$  on SIESTA.

## 6.2. Sleep Analyses

We asked the question “What is the impact of sleep on SIESTA’s ability to learn and remember?” These experiments are for incremental class learning, and data augmentation is not used. First, we analyze the pre-sleep and post-sleep performance of SIESTA on ImageNet-1K in Fig. 4 using the same sleep settings as in Sec. 6.1. We see that the performance of SIESTA after sleep is consistently higher than before sleep for all increments, providing a  $4.25 \pm 1.38\%$  average absolute increase in accuracy after each sleep cycle.

Next, we study the impact of sleep frequency. To do this, we trained models with a sleep frequency of 50, 100 (default), or 150 classes seen. For this analysis, we used a fixed sleep length, i.e., a fixed number of updates per sleep ( $m = 1.28M$ ). The absolute average increase in post-sleep accuracy was  $2.29 \pm 0.86\%$  for 50 classes,  $4.25 \pm 1.38\%$  for 100 classes, and  $6.18 \pm 2.15\%$  for 150 classes. Despite the 50 class increment being trained with more updates, the 100 class increment achieved better post-sleep performance. We hypothesize that this happens because frequent sleep leads to greater perturbation in the DNN’s weights, resulting in gradual forgetting of old memories.

In Fig. 5, we study the impact of sleep length on SIESTA’s performance by varying the number of updates ( $m$ ) during each sleep period, where SIESTA slept every 100 classes. We observe that as sleep length increases, SIESTA’s performance also increases; however, as the sleep length increases, SIESTA requires more updates and there are diminishing returns in terms of increases in accuracy, so we must strike a balance between accuracy and efficiency.

Table 2: Experimental results with state-of-the-art methods on ImageNet-1K. DER without pruning and DER with pruning are abbreviated as DER $\dagger$  and DER\*, respectively. The ( $\uparrow$ ) and ( $\downarrow$ ) indicate high and low values to reflect optimum performance respectively.  $\mathcal{P}$  is the number of parameters in millions,  $\mu$  is the average top-5 accuracy,  $\alpha$  is the final top-5 accuracy,  $\mathcal{M}$  is the total memory in GB, and  $\mathcal{U}$  is the total number of updates in millions. We include SIESTA with (Aug) and without (No Aug) augmentations. DER\* does not report  $\mathcal{P}$ , so we omit it.

Method	$\mathcal{P}(\downarrow)$	$\mu(\uparrow)$	$\alpha(\uparrow)$	$\mathcal{M}(\downarrow)$	$\mathcal{U}(\downarrow)$
E2E [9]	11.68	72.09	52.29	22.32	93.26
S-DER [45]	28.00	85.62	80.76	22.39	213.17
iCaRL [58]	11.68	63.70	44.00	22.32	79.94
BiC [73]	11.68	84.00	73.20	22.32	119.91
WA [78]	11.68	86.60	81.10	22.32	133.23
DER $\dagger$ [74]	116.89	88.17	82.86	22.74	213.17
DER* [74]	—	87.08	81.89	22.32	213.17
DyTox [18]	11.36	88.78	83.91	22.32	692.80
REMIND [23]	11.68	83.61	77.14	2.05	58.78
SIESTA (No Aug)	5.48	88.33	83.59	2.02	<b>11.53</b>
SIESTA (Aug)	<b>5.48</b>	<b>90.67</b>	<b>87.00</b>	<b>2.02</b>	57.60

## 6.3. State-of-the-Art Comparisons

To put our work in context with respect to existing methods, we compare SIESTA against recent incremental class learning methods on ImageNet-1K. All methods, except for SIESTA (No Aug), use augmentations and have a variety of different DNN architectures. SIESTA (Aug), which uses augmentations, used 6.4 million updates per sleep cycle ( $m = 6.4M$ ). With the exception of REMIND and SIESTA, we use published performance numbers for all methods. REMIND and SIESTA both use 2.05GB of memory for rehearsal and SwAV for pre-training. Additional details for the comparison algorithms are provided in Sec. S1.

Overall results are in Table 2 and Fig. 1. SIESTA performs best in average accuracy  $\mu$  and final accuracy  $\alpha$ , while having fewer DNN parameters  $\mathcal{P}$ , lower auxiliary memory usage  $\mathcal{M}$ , and fewer total updates  $\mathcal{U}$ . While REMIND uses the same amount of auxiliary memory and a similar number of DNN updates, SIESTA (Aug) outperforms REMIND by 10% (absolute) in final accuracy. SIESTA (Aug) exceeds DyTox, the method with the second highest final accuracy, by 3.08% (absolute), while using  $12\times$  fewer network updates and  $11\times$  less memory.

SIESTA (No Aug) has comparable performance to state of the art batch learners like DER and DyTox, while requiring  $18\times$  fewer updates. Moreover, SIESTA (Aug) can provide even further performance gains (3.41% absolute improvement in final accuracy) at the cost of  $5\times$  more updates.

## 6.4. Computational Analysis

We trained SIESTA on a single NVIDIA A5000 GPU. Excluding pre-training, training SIESTA on ImageNet-1K required only 2.4 hours using the configurations from Sec. 6.1 when augmentations were not used. On the same hardware, training SIESTA is  $3.4\times$  faster than REMIND. All methods use a comparable amount of auxiliary memory, where REMIND and SIESTA use it to store compressed tensors and the others use it to store 20,000 images.

For example, many existing models require a large number of parameters (11.68 – 116.89 million), DNN updates (79 – 692 million), and additional memory to store the current batch and/or to keep additional copies of the DNN in memory (22 gigabytes [9, 45, 58, 73, 78, 74, 18]). This makes these methods infeasible for on-device learning.

## 7. Discussion

This paper considers the problem of supervised continual learning, where the learner incrementally learns from a sequence about which it cannot make distributional assumptions. We argue that for real-world applications, continual learning needs to rival an offline learner and be more computationally efficient than periodically re-training from scratch. We also argue that systems need to be designed to handle arbitrary class orderings, where two extremes are iid and class-incremental learning, whereas many continual learning systems are bespoke to the incremental class learning scenario. We demonstrated that SIESTA largely meets these goals, achieving identical performance to the offline learner when augmentations are not used, and outperforming existing continual learning methods in accuracy using less compute when augmentations are used.

Computational efficiency in continual learning has long been a selling point of the research, but it has not been a focus of prior work. Training large DNNs from scratch requires a huge amount of energy that can result in a large amount of greenhouse gas emissions [53, 72]. From a financial perspective, training large models often requires a large amount of electricity, expensive hardware, and cloud computing resources. Many are calling for more computationally efficient algorithms to be developed [66, 68], and we believe that continual learning can help address this problem while also enabling greater functionality provided by continuously updating DNNs with new information.

Because one of the major applications for continual learning is on-device learning, we focused on mobile DNNs, which can enable devices to learn about their users and their environments in a way that provides greater privacy than relying on cloud computing. Learning on-device can also be useful in areas with poor internet connectivity. However, computational efficiency improvements are mostly needed for updating large DNNs, e.g., Foundation

Models [56, 56, 14], that have billions/trillions of parameters and can take months to train using thousands of GPUs.

In this work, we only evaluated CNN architectures with SIESTA; however, the general framework is amenable to other architectures as long as the representations can be quantized. For example, SIESTA could be extended for models like Swin Transformers [46] or even Graph Neural Networks [80], where we could quantize graph representations. Exploring the use of non-CNN architectures is critical for using SIESTA in non-vision modalities, e.g., audio and text data, which would be an exciting area of future work. Another interesting area of research could be incorporating additional data modalities over time to improve existing task performance and enhancing the learning of new tasks. Another direction is to use SIESTA for tasks such as continual learning in object detection, which was previously done using a REMIND-based system [2].

SIESTA depends on the initial layers of the network,  $\mathcal{H}$ , being universal features for the domain, since they are not trained after the base initialization phase. Following others [58, 6, 23], we did base initialization on the first 100 classes of ImageNet-1K. While our model rivaled the offline learner when augmentations were not used, there was a small gap when augmentations were used between SIESTA and the offline learner. We hypothesize that this gap would be closed by improving the features in  $\mathcal{H}$ . Two potential ways to achieve this goal would be using a superior self-supervised learning algorithm than SwAV or by training on additional data. For continual learning for real applications, it would be prudent to initialize the DNN from a very large unlabeled dataset with self-supervised learning, which would likely work significantly better.

We allowed methods to perform a pre-training phase, which was not included in the total number of updates. We argue that this is viable since pre-training only occurs once during a model’s lifetime, and by performing continual learning, a practitioner would not need to periodically re-train a model on new and old (pre-training) data. Future work should investigate the role of more performant self-supervised learning models for producing invariant features. Invariant features could reduce the need for augmentation during continual learning, further improving efficiency.

## 8. Conclusion

We proposed SIESTA, a scalable, faster and lightweight continual learning framework equipped with offline memory consolidation. We reduced computational overhead by making online learning free of rehearsal or expensive parametric updates during the wake phase. This closely aligns with real-time applications such as edge-devices, mobile phones, smart home appliances, robots, and virtual assistants. To effectively learn from a non-stationary data stream, the short-term wake memories were transferred into



the DNN for long-term storage during offline sleep periods. Consequently, our model overcame forgetting of past knowledge. We showed that sleep improved online performance while outperforming state-of-the-art methods. SIESTA achieves similar accuracy to DyTox [18] using an order of magnitude fewer updates when augmentations are not used, and surpasses DyTox in terms of accuracy when using augmentations. Although we evaluated SIESTA on image classification where augmentations are widely used, SIESTA can also be used for non-vision tasks where augmentations are not widely used.

**Acknowledgements.** We thank Robik Shrestha for providing comments on the manuscript. This work was supported in part by NSF awards #1909696 and #2047556. The views and conclusions contained herein are those of the authors and should not be interpreted as representing the official policies or endorsements of any sponsor.

## References

- [1] Wickliffe C Abraham and Anthony Robins. Memory retention—the synaptic stability versus plasticity dilemma. *Trends in neurosciences*, 28(2):73–78, 2005. 3
- [2] Manoj Acharya, Tyler L Hayes, and Christopher Kanan. Rodeo: Replay for online object detection. In *BMVC*, 2020. 8
- [3] Rahaf Aljundi, Francesca Babiloni, Mohamed Elhoseiny, Marcus Rohrbach, and Tinne Tuytelaars. Memory aware synapses: Learning what (not) to forget. In *Proceedings of the European Conference on Computer Vision (ECCV)*, pages 139–154, 2018. 3
- [4] Rahaf Aljundi, Lucas Caccia, Eugene Belilovsky, Massimo Caccia, Min Lin, Laurent Charlin, and Tinne Tuytelaars. On-line continual learning with maximally interfered retrieval. *arXiv preprint arXiv:1908.04742*, 2019. 3
- [5] Elahe Arani, Fahad Sarfraz, and Bahram Zonooz. Learning fast, learning slow: A general continual learning method based on complementary learning system. In *International Conference on Learning Representations*, 2022. 3
- [6] Eden Belouadah and Adrian Popescu. Il2m: Class incremental learning with dual memory. In *Proceedings of the IEEE/CVF International Conference on Computer Vision*, pages 583–592, 2019. 3, 8
- [7] Denise J Cai, Sarnoff A Mednick, Elizabeth M Harrison, Jennifer C Kanady, and Sara C Mednick. Rem, not incubation, improves creativity by priming associative networks. *Proceedings of the National Academy of Sciences*, 106(25):10130–10134, 2009. 3
- [8] Mathilde Caron, Ishan Misra, Julien Mairal, Priya Goyal, Piotr Bojanowski, and Armand Joulin. Unsupervised learning of visual features by contrasting cluster assignments. *arXiv preprint arXiv:2006.09882*, 2020. 5, S2
- [9] Francisco M Castro, Manuel J Marín-Jiménez, Nicolás Guil, Cordelia Schmid, and Karteek Alahari. End-to-end incremental learning. In *Proceedings of the European conference on computer vision (ECCV)*, pages 233–248, 2018. 2, 3, 5, 7, 8, S1
- [10] Arslan Chaudhry, Puneet K Dokania, Thalaiyasingam Ajanthan, and Philip HS Torr. Riemannian walk for incremental learning: Understanding forgetting and intransigence. In *Proceedings of the European Conference on Computer Vision (ECCV)*, pages 532–547, 2018. 3
- [11] Arslan Chaudhry, Marc’Aurelio Ranzato, Marcus Rohrbach, and Mohamed Elhoseiny. Efficient lifelong learning with a-gem. *arXiv preprint arXiv:1812.00420*, 2018. 2, 3
- [12] William Jay Conover. *Practical nonparametric statistics*, volume 350. John Wiley & sons, 1999. 6
- [13] Robert Coop, Aaron Mishtal, and Itamar Arel. Ensemble learning in fixed expansion layer networks for mitigating catastrophic forgetting. *IEEE transactions on neural networks and learning systems*, 24(10):1623–1634, 2013. 3
- [14] Jacob Devlin, Ming-Wei Chang, Kenton Lee, and Kristina Toutanova. Bert: Pre-training of deep bidirectional transformers for language understanding. *arXiv preprint arXiv:1810.04805*, 2018. 8
- [15] Prithviraj Dhar, Rajat Vikram Singh, Kuan-Chuan Peng, Ziyang Wu, and Rama Chellappa. Learning without memorizing. In *Proceedings of the IEEE/CVF Conference on Computer Vision and Pattern Recognition*, pages 5138–5146, 2019. 3
- [16] Ina Djonlagic, Andrew Rosenfeld, Daphna Shohamy, Catherine Myers, Mark Gluck, and Robert Stickgold. Sleep enhances category learning. *Learning & memory*, 16(12):751–755, 2009. 3
- [17] Arthur Douillard, Matthieu Cord, Charles Ollion, Thomas Robert, and Eduardo Valle. Podnet: Pooled outputs distillation for small-tasks incremental learning. In *Computer vision-ECCV 2020-16th European conference, Glasgow, UK, August 23-28, 2020, Proceedings, Part XX*, volume 12365, pages 86–102. Springer, 2020. 2
- [18] Arthur Douillard, Alexandre Ramé, Guillaume Couairon, and Matthieu Cord. Dytox: Transformers for continual learning with dynamic token expansion. *arXiv preprint arXiv:2111.11326*, 2021. 2, 3, 4, 5, 7, 8, 9, S1
- [19] Timothy J Draelos, Nadine E Miner, Christopher C Lamb, Jonathan A Cox, Craig M Vineyard, Kristofor D Carlson, William M Severa, Conrad D James, and James B Aimone. Neurogenesis deep learning: Extending deep networks to accommodate new classes. In *2017 International Joint Conference on Neural Networks (IJCNN)*, pages 526–533. IEEE, 2017. 3
- [20] Simon J Durrant, Scott A Cairney, Cathal McDermott, and Penelope A Lewis. Schema-conformant memories are preferentially consolidated during rem sleep. *Neurobiology of Learning and Memory*, 122:41–50, 2015. 3
- [21] Chrisantha Fernando, Dylan Banarse, Charles Blundell, Yori Zwols, David Ha, Andrei A Rusu, Alexander Pritzel, and Daan Wierstra. Pathnet: Evolution channels gradient descent in super neural networks. *arXiv preprint arXiv:1701.08734*, 2017. 2, 3
- [22] Robert M French. Pseudo-recurrent connectionist networks: An approach to the ‘sensitivity-stability’ dilemma. *Connection Science*, 9(4):353–380, 1997. 3

- [23] Jhair Gallardo, Tyler L Hayes, and Christopher Kanan. Self-supervised training enhances online continual learning. In *British Machine Vision Conference (BMVC)*, 2021. 3, 5, 7, 8, S1, S2
- [24] Siavash Golkar, Michael Kagan, and Kyunghyun Cho. Continual learning via neural pruning. *arXiv preprint arXiv:1903.04476*, 2019. 2
- [25] Tyler L Hayes, Nathan D Cahill, and Christopher Kanan. Memory efficient experience replay for streaming learning. In *2019 International Conference on Robotics and Automation (ICRA)*, pages 9769–9776. IEEE, 2019. 3
- [26] Tyler L Hayes, Kushal Kafle, Robik Shrestha, Manoj Acharya, and Christopher Kanan. Remind your neural network to prevent catastrophic forgetting. In *European Conference on Computer Vision*, pages 466–483. Springer, 2020. 2, 3, 4, 5, S1, S2
- [27] Tyler L Hayes and Christopher Kanan. Lifelong machine learning with deep streaming linear discriminant analysis. In *Proceedings of the IEEE/CVF Conference on Computer Vision and Pattern Recognition Workshops*, pages 220–221, 2020. 3, 5, S1
- [28] Tyler L Hayes and Christopher Kanan. Online continual learning for embedded devices. In *CoLLAs*, 2022. 5
- [29] Tyler L Hayes, Giri P Krishnan, Maxim Bazhenov, Hava T Siegelmann, Terrence J Sejnowski, and Christopher Kanan. Replay in deep learning: Current approaches and missing biological elements. *Neural Computation*, 33(11):2908–2950, 2021. 2, 3
- [30] P Hetherington. Is there ‘catastrophic interference’ in connectionist networks? In *Proceedings of the 11th annual conference of the cognitive science society*, pages 26–33. LEA, 1989. 2
- [31] Saihui Hou, Xinyu Pan, Chen Change Loy, Zilei Wang, and Dahua Lin. Lifelong learning via progressive distillation and retrospection. In *Proceedings of the European Conference on Computer Vision (ECCV)*, pages 437–452, 2018. 3
- [32] Saihui Hou, Xinyu Pan, Chen Change Loy, Zilei Wang, and Dahua Lin. Learning a unified classifier incrementally via rebalancing. In *Proceedings of the IEEE/CVF Conference on Computer Vision and Pattern Recognition*, pages 831–839, 2019. 2, 3
- [33] Andrew Howard, Mark Sandler, Grace Chu, Liang-Chieh Chen, Bo Chen, Mingxing Tan, Weijun Wang, Yukun Zhu, Ruoming Pang, Vijay Vasudevan, et al. Searching for mobilenetv3. In *Proceedings of the IEEE/CVF international conference on computer vision*, pages 1314–1324, 2019. 5
- [34] Ching-Yi Hung, Cheng-Hao Tu, Cheng-En Wu, Chien-Hung Chen, Yi-Ming Chan, and Chu-Song Chen. Compacting, picking and growing for unforgetting continual learning. *Advances in Neural Information Processing Systems*, 32, 2019. 2
- [35] Herve Jegou, Matthijs Douze, and Cordelia Schmid. Product quantization for nearest neighbor search. *IEEE transactions on pattern analysis and machine intelligence*, 33(1):117–128, 2010. 4
- [36] Jeff Johnson, Matthijs Douze, and Hervé Jégou. Billion-scale similarity search with gpus. *IEEE Transactions on Big Data*, 2019. 5
- [37] Minsoo Kang, Jaeyoo Park, and Bohyung Han. Class-incremental learning by knowledge distillation with adaptive feature consolidation. In *Proceedings of the IEEE/CVF conference on computer vision and pattern recognition*, pages 16071–16080, 2022. 3
- [38] Ronald Kemker and Christopher Kanan. Fearnnet: Brain-inspired model for incremental learning. In *ICLR*, 2018. 3
- [39] Ronald Kemker, Marc McClure, Angelina Abitino, Tyler Hayes, and Christopher Kanan. Measuring catastrophic forgetting in neural networks. In *Proceedings of the AAAI Conference on Artificial Intelligence*, 2018. 1, 3
- [40] James Kirkpatrick, Razvan Pascanu, Neil Rabinowitz, Joel Veness, Guillaume Desjardins, Andrei A Rusu, Kieran Milan, John Quan, Tiago Ramalho, Agnieszka Grabska-Barwinska, et al. Overcoming catastrophic forgetting in neural networks. *Proceedings of the national academy of sciences*, 114(13):3521–3526, 2017. 3
- [41] Simon Kornblith, Ting Chen, Honglak Lee, and Mohammad Norouzi. Why do better loss functions lead to less transferable features? *Advances in Neural Information Processing Systems*, 34:28648–28662, 2021. 4
- [42] Penelope A. Lewis, Günther Knoblich, and Gina Poe. How Memory Replay in Sleep Boosts Creative Problem-Solving. *Trends in Cognitive Sciences*, 22(6):491–503, June 2018. 3
- [43] Wei Li, Lei Ma, Guang Yang, and Wen-Biao Gan. Rem sleep selectively prunes and maintains new synapses in development and learning. *Nature neuroscience*, 20(3):427–437, 2017. 3
- [44] Zhizhong Li and Derek Hoiem. Learning without forgetting. *IEEE transactions on pattern analysis and machine intelligence*, 40(12):2935–2947, 2017. 3
- [45] Zhuoyun Li, Changhong Zhong, Sijia Liu, Ruixuan Wang, and Wei-Shi Zheng. Preserving earlier knowledge in continual learning with the help of all previous feature extractors. *arXiv preprint arXiv:2104.13614*, 2021. 5, 7, 8, S1
- [46] Ze Liu, Yutong Lin, Yue Cao, Han Hu, Yixuan Wei, Zheng Zhang, Stephen Lin, and Baining Guo. Swin transformer: Hierarchical vision transformer using shifted windows. In *Proceedings of the IEEE/CVF international conference on computer vision*, pages 10012–10022, 2021. 8
- [47] Ziwei Liu, Zhongqi Miao, Xiaohang Zhan, Jiayun Wang, Boqing Gong, and Stella X Yu. Large-scale long-tailed recognition in an open world. In *Proceedings of the IEEE/CVF conference on computer vision and pattern recognition*, pages 2537–2546, 2019. S2
- [48] David Lopez-Paz and Marc’Aurelio Ranzato. Gradient episodic memory for continual learning. *arXiv preprint arXiv:1706.08840*, 2017. 3
- [49] James L McClelland and Nigel H Goddard. Considerations arising from a complementary learning systems perspective on hippocampus and neocortex. *Hippocampus*, 6(6):654–665, 1996. 2
- [50] Thomas Mensink, Jakob Verbeek, Florent Perronnin, and Gabriela Csurka. Distance-based image classification: Generalizing to new classes at near-zero cost. *IEEE transactions on pattern analysis and machine intelligence*, 35(11):2624–2637, 2013. 5

- [51] Oleksiy Ostapenko, Mihai Puscas, Tassilo Klein, Patrick Jah-nichen, and Moin Nabi. Learning to remember: A synaptic plasticity driven framework for continual learning. In *Proceedings of the IEEE/CVF Conference on Computer Vision and Pattern Recognition*, pages 11321–11329, 2019. [3](#)
- [52] German I Parisi, Ronald Kemker, Jose L Part, Christopher Kanan, and Stefan Wermter. Continual lifelong learning with neural networks: A review. *Neural Networks*, 113:54–71, 2019. [1](#)
- [53] David Patterson, Joseph Gonzalez, Quoc Le, Chen Liang, Lluis-Miquel Munguia, Daniel Rothchild, David So, Maud Texier, and Jeff Dean. Carbon emissions and large neural network training. *arXiv preprint arXiv:2104.10350*, 2021. [8](#)
- [54] Quang Pham, Chenghao Liu, and Steven Hoi. Dualnet: Continual learning, fast and slow. *Advances in Neural Information Processing Systems*, 34:16131–16144, 2021. [3](#)
- [55] Quang Pham, Chenghao Liu, Doyen Sahoo, and Steven Hoi. Learning fast and slow for time series forecasting. In *The Eleventh International Conference on Learning Representations*, 2023. [3](#)
- [56] Alec Radford, Jong Wook Kim, Chris Hallacy, Aditya Ramesh, Gabriel Goh, Sandhini Agarwal, Girish Sastry, Amanda Askell, Pamela Mishkin, Jack Clark, et al. Learning transferable visual models from natural language supervision. In *International conference on machine learning*, pages 8748–8763. PMLR, 2021. [8](#)
- [57] Jathushan Rajasegaran, Munawar Hayat, Salman H Khan, Fahad Shahbaz Khan, and Ling Shao. Random path selection for continual learning. *Advances in Neural Information Processing Systems*, 32, 2019. [2](#)
- [58] Sylvestre-Alvise Rebuffi, Alexander Kolesnikov, Georg Sperl, and Christoph H Lampert. icarl: Incremental classifier and representation learning. In *Proceedings of the IEEE conference on Computer Vision and Pattern Recognition*, pages 2001–2010, 2017. [2](#), [3](#), [5](#), [7](#), [8](#), [S1](#)
- [59] Hippolyt Ritter, Aleksandar Botev, and David Barber. On-line structured laplace approximations for overcoming catastrophic forgetting. *arXiv preprint arXiv:1805.07810*, 2018. [3](#)
- [60] Olga Russakovsky, Jia Deng, Hao Su, Jonathan Krause, Sanjeev Satheesh, Sean Ma, Zhiheng Huang, Andrej Karpathy, Aditya Khosla, Michael Bernstein, et al. Imagenet large scale visual recognition challenge. *International journal of computer vision*, 115(3):211–252, 2015. [6](#)
- [61] Andrei A Rusu, Neil C Rabinowitz, Guillaume Desjardins, Hubert Soyer, James Kirkpatrick, Koray Kavukcuoglu, Razvan Pascanu, and Raia Hadsell. Progressive neural networks. *arXiv preprint arXiv:1606.04671*, 2016. [3](#)
- [62] Joan Serra, Didac Suris, Marius Miron, and Alexandros Karatzoglou. Overcoming catastrophic forgetting with hard attention to the task. In *International Conference on Machine Learning*, pages 4548–4557. PMLR, 2018. [2](#), [3](#)
- [63] Carlyle Smith and Danielle Smith. Ingestion of ethanol just prior to sleep onset impairs memory for procedural but not declarative tasks. *Sleep*, 26(2):185–191, 2003. [3](#)
- [64] Leslie N Smith and Nicholay Topin. Super-convergence: Very fast training of neural networks using large learning rates. *arxiv. arXiv preprint arXiv:1708.07120*, 2017. [6](#)
- [65] Ben Sorscher, Robert Geirhos, Shashank Shekhar, Surya Ganguli, and Ari S Morcos. Beyond neural scaling laws: beating power law scaling via data pruning. *arXiv preprint arXiv:2206.14486*, 2022. [S4](#), [S5](#)
- [66] Emma Strubell, Ananya Ganesh, and Andrew McCallum. Energy and policy considerations for modern deep learning research. In *Proceedings of the AAAI Conference on Artificial Intelligence*, volume 34, pages 13693–13696, 2020. [8](#)
- [67] Xiaoyu Tao, Xinyuan Chang, Xiaopeng Hong, Xing Wei, and Yihong Gong. Topology-preserving class-incremental learning. In *European Conference on Computer Vision*, pages 254–270. Springer, 2020. [2](#), [3](#)
- [68] Aimee Van Wynsberghe. Sustainable ai: Ai for sustainability and the sustainability of ai. *AI and Ethics*, 1(3):213–218, 2021. [8](#)
- [69] Vikas Verma, Alex Lamb, Christopher Beckham, Amir Najafi, Ioannis Mitliagkas, David Lopez-Paz, and Yoshua Bengio. Manifold mixup: Better representations by interpolating hidden states. In *International conference on machine learning*, pages 6438–6447. PMLR, 2019. [5](#)
- [70] Albrecht P Vorster and Jan Born. Sleep and memory in mammals, birds and invertebrates. *Neuroscience & Biobehavioral Reviews*, 50:103–119, 2015. [2](#)
- [71] Kai Wang, Joost van de Weijer, and Luis Herranz. Acaeremind for online continual learning with compressed feature replay. *Pattern Recognition Letters*, 150:122–129, 2021. [3](#)
- [72] Carole-Jean Wu, Ramya Raghavendra, Udit Gupta, Bilge Acun, Newsha Ardalani, Kiwan Maeng, Gloria Chang, Fiona Aga, Jinshi Huang, Charles Bai, et al. Sustainable ai: Environmental implications, challenges and opportunities. *Proceedings of Machine Learning and Systems*, 4:795–813, 2022. [8](#)
- [73] Yue Wu, Yinpeng Chen, Lijuan Wang, Yuancheng Ye, Zicheng Liu, Yandong Guo, and Yun Fu. Large scale incremental learning. In *Proceedings of the IEEE/CVF Conference on Computer Vision and Pattern Recognition*, pages 374–382, 2019. [2](#), [3](#), [5](#), [7](#), [8](#), [S1](#)
- [74] Shipeng Yan, Jiangwei Xie, and Xuming He. Der: Dynamically expandable representation for class incremental learning. In *Proceedings of the IEEE/CVF Conference on Computer Vision and Pattern Recognition*, pages 3014–3023, 2021. [2](#), [3](#), [5](#), [7](#), [8](#), [S1](#), [S2](#)
- [75] Jaehong Yoon, Eunho Yang, Jeongtae Lee, and Sung Ju Hwang. Lifelong learning with dynamically expandable networks. *arXiv preprint arXiv:1708.01547*, 2017. [3](#)
- [76] Sangdoo Yun, Dongyoon Han, Seong Joon Oh, Sanghyuk Chun, Junsuk Choe, and Youngjoon Yoo. Cutmix: Regularization strategy to train strong classifiers with localizable features. In *Proceedings of the IEEE/CVF international conference on computer vision*, pages 6023–6032, 2019. [5](#)
- [77] Friedemann Zenke, Ben Poole, and Surya Ganguli. Continual learning through synaptic intelligence. In *International Conference on Machine Learning*, pages 3987–3995. PMLR, 2017. [3](#)
- [78] Bowen Zhao, Xi Xiao, Guojun Gan, Bin Zhang, and Shu-Tao Xia. Maintaining discrimination and fairness in class incremental learning. In *Proceedings of the IEEE/CVF Con-*

*ference on Computer Vision and Pattern Recognition*, pages 13208–13217, 2020. [2](#), [5](#), [7](#), [8](#), [S1](#)

- [79] Bolei Zhou, Agata Lapedriza, Aditya Khosla, Aude Oliva, and Antonio Torralba. Places: A 10 million image database for scene recognition. *IEEE transactions on pattern analysis and machine intelligence*, 40(6):1452–1464, 2017. [S2](#)
- [80] Jie Zhou, Ganqu Cui, Shengding Hu, Zhengyan Zhang, Cheng Yang, Zhiyuan Liu, Lifeng Wang, Changcheng Li, and Maosong Sun. Graph neural networks: A review of methods and applications. *AI open*, 1:57–81, 2020. [8](#)



## Supplemental Material

We organize additional supporting experimental findings as follows: Sec. S1 contains brief descriptions of the compared methods. The implementation details about SIESTA, REMIND, and DER are included in Sec. S2. An analysis on rehearsal policies is located in Sec. S3. We compare offline MobileNetV3-L with offline ResNet18 in Sec. S4, and we analyze MobileNet quantization layers in Sec. S5. A comparison with the offline model when augmentations are used can be found in Sec. S6. Sec. S7 describes online learning results when sleep is omitted. For SIESTA, we study the impact of buffer size in Sec. S8 and batch size in Sec. S9. Finally, we include additional computational analysis in Sec. S10.

### S1. Comparison Algorithms

This paper compared SIESTA’s performance against state-of-the-art continual learning algorithms, including:

- **REMIND [26]**: Instead of veridical replay (i.e., raw pixels), REMIND performs representation replay using mid-level CNN features that are compressed by PQ. This significantly reduces memory and enables REMIND to store more examples to mitigate catastrophic forgetting. It keeps earlier CNN layers fixed for feature extraction and trains later plastic layers for classification. Another variant of REMIND [23] replaces supervised pretraining by self-supervised pretraining and improves REMIND’s performance.
- **SLDA [27]**: SLDA learns only the final classification layer while keeping earlier pretrained CNN layers fixed. It stores separate mean vectors for each class and a shared covariance matrix; only these class statistics are updated during online training and used for predictions.
- **iCaRL [58]**: iCaRL performs incremental batch learning using veridical replay (i.e., raw pixels). It utilizes distillation loss and a nearest class mean classifier to prevent catastrophic forgetting.
- **BiC [73]**: BiC builds on iCaRL and also uses distillation loss and replay. It introduces a bias correction mechanism to prevent bias from class imbalance. For that, a linear model is learned on validation data to recalibrate the model’s probabilities.
- **WA [78]**: WA applies a knowledge distillation loss and a bias correction step where it aligns the norms of new class weights to those of old class weights.
- **End-to-End [9]**: End-to-End is a variant of iCaRL. Instead of the nearest class mean classifier, it utilizes the CNN’s output layer.

- **DER [74]**: By reusing previous feature extractors, DER freezes previously learned representations and augments them with incoming features obtained from a newly trained feature extractor. It employs a channel-level mask-based pruning mechanism to dynamically expand representations. It uses an auxiliary classifier along with a regular classifier to discriminate between old and new concepts. In this paper, we compare with two variants of DER: DER without pruning (referred to as DER<sup>†</sup>) and DER with pruning (referred to as DER<sup>\*</sup>). We also compare with a previous version referred to as S-DER [45] which also combines multiple feature extractors and applies pruning. However, S-DER still has  $2.4\times$  more parameters than offline ResNet18.

- **DyTox [18]**: DyTox is a Transformer-based encoder/decoder framework where the encoder and decoder are shared among tasks. Unlike DER which keeps a copy of the whole network per task, DyTox proposes a dynamic task token expansion method to adapt to new tasks. Thus it alleviates the issues of a) expanding the network parameters to scale and b) requiring task identifiers in dynamic expansion methods.

- **Nearest Class Mean (NCM)**: NCM computes a running mean for each class. During test time, a test sample is given the label of the nearest class mean. It becomes a variant of SLDA if the covariance matrix is fixed to the identity matrix.

- **Offline**: The offline model has access to the entire dataset and is trained using conventional batch training with multiple epochs. It serves as an approximate upper bound for an online learning model.

Veridical replay based methods apply various image augmentations. For example, BiC and DER use random crops and horizontal flips, while DyTox uses Rand-Augment. REMIND uses feature augmentation by doing random crops and mixup directly on the stored mid-level features. To compare continual learning methods, rather than augmentation strategies, our experiments in Sec. 6.1 omitted augmentations during the continual learning phase for SIESTA, REMIND, and DER. This allowed us to compare these algorithms in a fair way, where we also used the same DNN architecture.

### S2. Additional Implementation Details

#### S2.1. MobileNetV3-L

We use a slightly modified version of MobileNetV3-L with SIESTA, DER, and REMIND. We use the GELU activation instead of ReLU and Hard Swish in all

MobileNetV3-L layers, except for the squeeze and excitation block. We replace batch normalization with group normalization and weight standardization in the  $\mathcal{F}$  and  $\mathcal{G}$  layers. We used GELU activation because it improves gradient flow. And, we used group normalization with weight standardization because they are effective for small batch-sizes while performing competitively to batch normalization for large batch-sizes. We incorporate these architectural modifications into MobileNetV3-L to get rid of adverse effects of batch normalization and make the model more general purpose.

The offline MobileNetV3-L was trained for 600 epochs using the AdamW optimizer with an initial LR of 0.004 and a weight decay of 0.05. We used the Cosine Annealing LR scheduler with a linear warm up of 5 epochs.

## S2.2. Base Initialization

SIESTA, REMIND, and DER are initialized using all images in the first batch of 100 classes from ImageNet-1K, which is referred to as “base initialization.” We use the same data ordering as REMIND [26]. Base initialization consists of three phases:

1. Following [23], we first perform self-supervised pre-training of the network using SwAV. We use the small batch procedure from the original SwAV paper [8]. Following others who have used self-supervised learning with mobile DNNs, we modified the scale of global and local crops in multi-crop augmentation. We use  $2 \times 224 + 6 \times 128$  crops with a minimum scale crop range of  $[0.3 - 0.05]$  and maximum scale crop range of  $[1.0 - 0.3]$ . We use 1000 prototypes, a Sinkhorn regularization parameter  $\epsilon$  of 0.03, queue length of 384 features, and 2000 epochs. We set the base LR to 0.6, final LR to 0.0006, and batch size to 64. The remaining settings are identical to the original SwAV [8] system.
2. For REMIND and SIESTA only, we then fit the parameters of the product quantization algorithm OPQ to the embeddings produced by  $\mathcal{H}$ . OPQ is configured to use 8 codebooks of size 256. In our main results,  $\mathcal{H}$  consists of the first 8 layers of the DNN.
3. Supervised fine-tuning is then done on the DNN, where for DER the entire network is trained, but for REMIND and SIESTA only  $\mathcal{F}$  and  $\mathcal{G}$  are trained using the reconstructed tensors from  $\mathcal{H}$ . For DER, we use the SGD optimizer with an initial LR of 0.1 which is decayed by a 0.1 multiplier every 15 epochs. We use 50 epochs and the standard PyTorch augmentations (random resized crop and random horizontal flip) for training DER. For SIESTA and REMIND, we train for 50 epochs. SGD is used for optimization with an initial LR of 0.2 for the last layer and a LR of 0.07 for the remaining layers. The LR is decayed by a 0.1 multiplier

every 15 epochs. REMIND uses augmentations found optimum in the original REMIND paper [26]. SIESTA uses Cutmix and Mixup. These augmentations are applied using participation probability  $p_{cutmix} = 0.6$  and  $p_{mixup} = 0.4$ . We set  $\beta = 1.0$  for Cutmix and  $\alpha = 0.1$  for Mixup.

After base-initialization, DER achieves 96.90% top-5 accuracy and REMIND/SIESTA achieve 96.84% top-5 accuracy on the validation set for the first 100 classes.

## S2.3. SIESTA

SIESTA’s settings for training during continual learning are described in Sec. 5.

## S2.4. REMIND

In our augmentation-free experiments, we configured REMIND to use the same number of updates as SIESTA (11.53M), which was done by setting REMIND to use a replay mini-batch size of 9.

In our augmentation experiments, we used REMIND’s default configuration, which uses a replay mini-batch size of 50. For these experiments, REMIND uses the same augmentation scheme as in the original REMIND paper.

## S2.5. DER

For our experiments without augmentations, we configured DER to use a similar number of updates as SIESTA and REMIND. To do this, we set the number of epochs used during each 100 class increment to 10. We adjusted the LR scheduler accordingly. In experiments with augmentations, DER used 47 epochs in every 100 class increment and random resized crop and random horizontal flip augmentations. Other implementation details e.g., optimizer and fine-tuning of the unified classifier follow the original DER paper [74]. In all experiments, DER stored 10 MobileNetV3-L models for 10 learning steps, the current batch of at least 100000 images, and a replay buffer of 10000 images ( $224 \times 224$  uint8); all of which required 20.99 GB in memory.

## S3. Rehearsal Policies

Since real-world data distribution is often long-tailed (LT) and imbalanced, we investigate the robustness of SIESTA and REMIND to LT data distribution using Places-LT dataset [47]. It is a long tailed variant of the Places-2 dataset [79]. It has a total of 365 categories with 62500 training images ranging from 5 to 4980 images per class. We use the Places-LT validation set from [47] as our test set consisting of a total of 7300 images with a balanced distribution of 20 images per class.

Since Places-LT is a small dataset, we first initialized all MobileNetV3-L layers with SwAV weights pre-trained on ImageNet base initialization subset i.e., 100 classes. Next

Table S1: Places-LT experimental results without augmentation. Symbols ( $\uparrow$ ) and ( $\downarrow$ ) indicate high and low values to reflect optimum results.  $\mu$  (average top-1 accuracy),  $\alpha$  (final top-1 accuracy),  $\mathcal{U}$  (total number of updates in Million). We show the mean  $\pm$  standard deviation across 5 different class incremental orderings. SIESTA $\dagger$  is a variant with uniform sampling, while SIESTA is our main method with balanced uniform sampling.

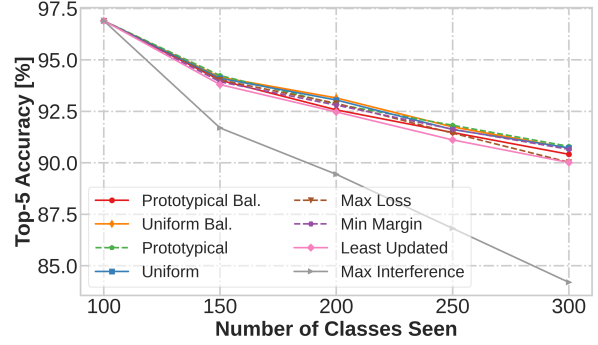
Methods	$\mu(\uparrow)$	$\alpha(\uparrow)$	$\mathcal{U}(\downarrow)$
Offline	—	22.49	2.50
REMIND	25.98 $\pm$ 1.10	17.00 $\pm$ 0.54	0.28
SIESTA $\dagger$	29.08 $\pm$ 1.30	20.15 $\pm$ 0.41	<b>0.23</b>
<b>SIESTA</b>	<b>33.35 <math>\pm</math> 1.22</b>	<b>24.88 <math>\pm</math> 0.46</b>	<b>0.23</b>

we fine-tuned the  $\mathcal{F}$  and  $\mathcal{G}$  layers using Places-LT base initialization subset i.e., 65 randomly chosen classes. The fine-tuning phase uses the same configuration as our ImageNet experiments. After that, the remaining 300 classes are learned incrementally in a total of 6 steps where each step consists of 50 classes. SIESTA uses 38400 updates per sleep cycle and REMIND uses 5 replay samples. The total number of updates for end-to-end training is bounded by 0.28M. The Offline model is initialized with SwAV weights and trained for 40 epochs using the same configuration as the ImageNet fine-tuning phase. Other implementation details follow ImageNet experiments with augmentation-free settings.

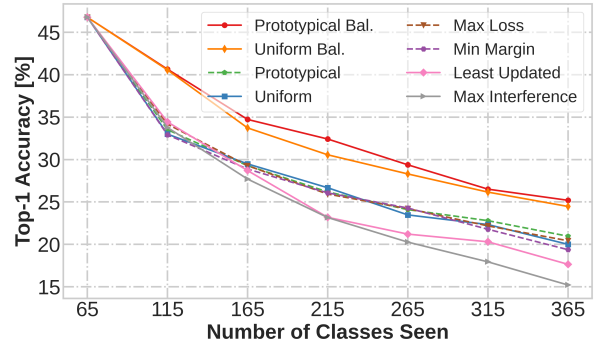
Table S1 compares SIESTA with REMIND in terms of mean  $\pm$  standard deviation across 5 different random class orderings on Places-LT. SIESTA $\dagger$  uses uniform sampling, while SIESTA uses uniform balanced sampling (balanced per class). We see that SIESTA $\dagger$  outperforms REMIND in terms of final and average accuracy and shows greater robustness than REMIND to Places-LT. Additionally, we see that the final accuracy has a low standard deviation ( $< 1\%$ ), demonstrating that REMIND and SIESTA $\dagger$  are robust against different data orderings. Also, we see that SIESTA with balanced uniform sampling (SIESTA) provides the highest accuracy, demonstrating its robustness to class imbalance.

After validating that balanced uniform sampling was superior to uniform sampling on Places-LT, we studied additional rehearsal sampling strategies on both balanced (ImageNet-1K) and long-tailed (Places-LT) distributions. For these experiments only 300 classes from ImageNet were used, where 200 were learned continually. We evaluated the following sampling policies:

- *Balanced Uniform*: Sampling each class uniformly, so that each has the same number of samples. This is used in our main results.
- *Uniform*: Sampling uniformly regardless of category.



(a) ImageNet



(b) Places-LT

Figure S1: Rehearsal policy analysis on: (a) ImageNet 300 classes (b) Places-LT 365 classes.

- *Least Updated*: Examples are prioritized based on how many times they contribute to updating DNN parameters so that the DNN does not forget about the examples with least counts.
- *Max Interference*: Samples having different class boundaries may interfere with one another due to the similarity or proximity in embedded space. These interfered samples may provide optimum supervision to improve performance. Interference is computed based on cosine similarity among penultimate features.
- *Max Loss*: Samples that the network is most uncertain about may better optimize the training objective. One way to implement this is by prioritizing samples that have the highest cross-entropy loss.
- *Min Margin*: The minimum margin policy prioritizes samples based on the separation between the highest and second highest probabilities given by the DNN. Lower separation corresponds to higher uncertainty and higher sampling probability.
- *Prototypical*: Samples closest to the respective class means are the most prototypical (i.e., class representative) whereas samples furthest from class means are the least prototypical. Giving higher priority to the most represen-

tative examples and lower priority to the least representative examples may improve learning that class.

- *Balanced Prototypical*: Selects equal number of samples per class using the prototypical criterion.

Since the standard deviation across orderings is low (see Table S1), we compare different policies based on a single ordering.

Results with different sampling policies are summarized in Fig. S1. Only the balanced uniform sampling policy was effective for both datasets. On ImageNet (Fig. S1a), we found that most of the replay methods perform similarly except max interference, which performs poorly. Max interference replays hard examples which is detrimental for small models [65]. In contrast, on Places-LT (Fig. S1b) we observed that balanced prototypical and balanced uniform performed best. We selected balanced uniform for our main results due to its simplicity and because it was effective across dataset label distributions.

## S4. Architecture Comparisons

The goal of this study is to find an optimum network architecture for efficient continual learning. Here we compare MobileNetV3-Large with ResNet18 to examine which architecture produces more universal features in the bottom network layers,  $\mathcal{H}$ . To do this, we pre-train  $\mathcal{H}$  using SwAV on the same pre-train set for both networks. We then train the top layers  $\mathcal{G}$  and output layer  $\mathcal{F}$  on ImageNet-1K in an offline way on reconstructed features from  $\mathcal{H}$ . The compression locations in both models maintain the same spatial dimension of  $14 \times 14$ . Since ResNet18 has a larger channel dimension (256) than MobileNetV3-L (80), the compression error is relatively higher in ResNet18.

Table S2 depicts comparisons with augmentations and without augmentation. In both cases, MobileNetV3-L features yield better accuracy than ResNet18 features. Therefore, MobileNetV3-L produces more generalizable features than ResNet18. Furthermore, MobileNetV3-L requires  $1.9\times$  fewer parameters than ResNet18. This comparison validates our rationale for choosing MobileNetV3-L.

## S5. MobileNet Quantization Layer

In Table S3, we examined SIESTA’s utility (parameters and memory) and performance (accuracy and compression error) for various MobileNet quantization layers. We maintained identical OPQ configurations for this analysis. As we move quantization layer up towards input, SIESTA’s accuracy increases due to increase in trainable parameters and OPQ quantization error decreases due to decrease in channel dimension. However, the increase in accuracy comes at a cost of increased memory. Since spatial dimension in upper layers increases, the memory requirement increases due to increased number of vectors corresponding to larger spa-

Table S2: Offline comparison training only  $\mathcal{F}$  and  $\mathcal{G}$  on quantized features from  $\mathcal{H}$  for MobileNetV3-Large and ResNet18 on ImageNet-1K. The ( $\uparrow$ ) and ( $\downarrow$ ) indicate high and low values to reflect optimum results respectively.  $\mathcal{P}$ ,  $\alpha$ , and  $\mathcal{E}_{OPQ}$  indicate the number of trainable parameters in millions, final top-5 accuracy (%), and OPQ quantization error, respectively.

Architecture	Augment	$\mathcal{P}(\downarrow)$	$\alpha(\uparrow)$	$\mathcal{E}_{OPQ}(\downarrow)$
ResNet18	✓	10.08	82.63	0.40
MobileNetV3-L	✓	<b>5.36</b>	<b>86.47</b>	<b>0.18</b>
ResNet18	×	10.08	79.54	0.40
MobileNetV3-L	×	<b>5.36</b>	<b>84.57</b>	<b>0.18</b>

Table S3: SIESTA’s performance as a function of quantization layer based on ImageNet-1K without augmentation. Here,  $\mathcal{S}$  is the tensor size ( $r \times s \times d$ ),  $\mathcal{P}$  is the number of trainable parameters in millions,  $\mathcal{M}$  is the memory consumption in GB,  $\mu$  is the average top-5 accuracy (%),  $\alpha$  is the final top-5 accuracy (%), and  $\mathcal{E}_{OPQ}$  indicates the OPQ quantization error. The ( $\uparrow$ ) and ( $\downarrow$ ) indicate high and low values to reflect optimum performance respectively.

Layer	$\mathcal{S}$	$\mathcal{P}(\downarrow)$	$\mathcal{M}(\downarrow)$	$\mu(\uparrow)$	$\alpha(\uparrow)$	$\mathcal{E}_{OPQ}(\downarrow)$
3	$56^2 \times 24$	5.47	32.19	89.39	85.18	0.03
5	$28^2 \times 40$	5.46	8.08	89.16	84.68	0.07
8	$14^2 \times 80$	5.36	2.05	88.33	83.59	0.18
14	$7^2 \times 160$	4.26	0.55	85.37	79.69	0.35

tial dimension. For example, spatial dimension in layer 5 is  $2\times$  larger than that in layer 8, hence memory required to store features in layer 5 becomes  $4\times$  more than layer 8. The opposite is true when moving quantization layer down towards output. To balance accuracy and efficiency we select layer 8 for all our experiments in the main results. Layer 8 provides suitable tensor size to meet lower memory budget while maintaining optimum accuracy.

## S6. Comparison with the Offline Learner when Augmentations are Used

In Table S4, we compare SIESTA with REMIND and DER under identical settings where all methods use MobileNetV3-L, SwAV pre-training, same number of updates, and augmentations. SIESTA outperforms DER by 15.18% (absolute) in final accuracy while using  $10\times$  less memory and  $10\times$  fewer parameters. While SIESTA uses same number of parameters and same amount of memory as REMIND, it outperforms REMIND by 4.03% (absolute) in final accuracy. When comparing to the offline learner, SIESTA has the smallest gap (3.74% absolute) in terms of final accuracy.

Using McNemar’s test to compare SIESTA’s final top-5 accuracy in the iid and class incremental setting, there was



Table S4: Experimental results with augmentations based on ImageNet-1K. We constrain methods to 58.8M updates but allow them to use their own augmentation settings. The ( $\uparrow$ ) and ( $\downarrow$ ) indicate high and low values to reflect optimum performance respectively.  $\mathcal{P}$  is the number of parameters in Millions,  $\mu$  is the average top-5 accuracy,  $\alpha$  is the final top-5 accuracy,  $\mathcal{M}$  is the total memory in GB, and  $\mathcal{U}$  is the total number of updates in Millions.

Method	$\mathcal{P}(\downarrow)$	$\mu(\uparrow)$	$\alpha(\uparrow)$	$\mathcal{M}(\downarrow)$	$\mathcal{U}(\downarrow)$
Offline	5.48	—	90.74	192.87	753.33
DER	54.80	82.72	71.82	20.99	58.39
REMIND	5.48	87.67	82.97	2.02	58.78
<b>SIESTA</b>	<b>5.48</b>	<b>90.67</b>	<b>87.00</b>	<b>2.02</b>	<b>57.60</b>

no significant difference in the accuracy of the two systems ( $P = 0.85$ ). Thus, SIESTA appears to be invariant to the order of the data when augmentations are used, which is consistent with our findings from Sec. 6.1 without augmentations. Using a McNemar’s test, we observed that there was a significant difference between the offline model and SIESTA when augmentations were used for both orderings ( $P < 0.001$ ). This is in contrast to our results without augmentations, where we found no significant difference. There are several routes that we believe are promising for closing this gap. These include using self-supervised learning methods that outperform SwAV, using additional capacity in  $\mathcal{H}$ , and developing additional augmentation techniques that could be used with the reconstructed tensors.

## S7. Online Learning Comparisons

In Fig. S2, we show learning curves on ImageNet-1K comparing online learning methods with an awake-only variant of SIESTA, which does not perform sleep steps. SIESTA (Awake Only) is an online learning method that updates  $\mathcal{F}$  as described in Sec. 4.1. From Fig. S2, we can see that SIESTA (Awake Only) rivals popular online learning methods NCM and SLDA, whereas with sleep it vastly outperforms them. All models use the same SwAV pre-trained DNN.

## S8. Impact of Buffer Size

In Table S5 we studied SIESTA’s performance as we altered the size of the buffer. We kept the total number of updates during a sleep cycle constant, which is consistent with observations in the dataset pruning literature that even when using pruned datasets a comparable number of updates are necessary to get equivalent performance in a neural network [65]. We see that SIESTA performs remarkably with smaller buffer size. The drop in final accuracy while changing buffer size from 2.01 GB to 0.75 GB is only 3.02% (absolute).

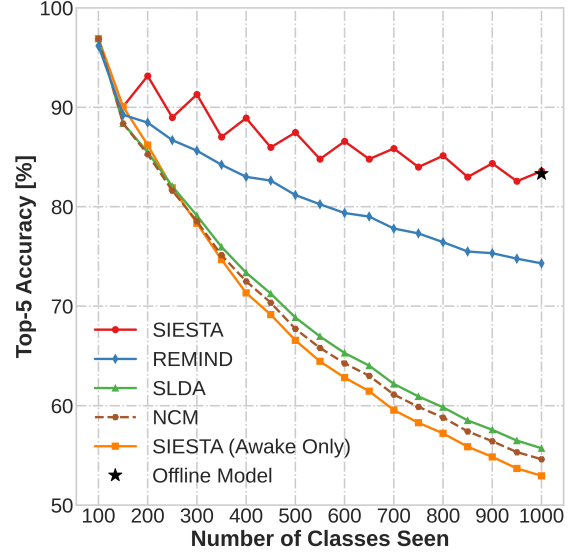


Figure S2: Learning curves for online continual learners without augmentations evaluated on ImageNet-1K. SIESTA (Awake Only) is an online variant of SIESTA that does not perform sleep.

Table S5: Impact of buffer size on SIESTA’s performance evaluated on ImageNet-1K without augmentation. The ( $\uparrow$ ) and ( $\downarrow$ ) indicate high and low values to reflect optimum performance respectively.  $\mu$  and  $\alpha$  denote average top-5 accuracy (%) and final top-5 accuracy (%), respectively. Buffer size is reported in GB.

Buffer Size	Quantized Instances	$\mu(\uparrow)$	$\alpha(\uparrow)$
0.75	479665	87.33	80.57
1.51	959665	88.30	83.30
2.01	1281167	88.33	83.59

## S9. Batchsize and Training Time for SIESTA

In Table S6 we studied SIESTA’s performance as we varied the batch size in offline training during sleep. We kept the total number of updates during a sleep cycle constant. We conducted the experiments on same hardware (NVIDIA RTX A5000 GPU). SIESTA shows robustness to varying batch size where it performs almost similarly for batch size ranges from 32 to 512. Increasing batch size provides a speed up, where a batch size of 512 requires  $2\times$  less time than batch size 32 to finish ImageNet-1K training.

## S10. Additional Computational Analysis

In the main text, to assess the computational efficiency of the continual learning algorithms we used the number of updates via backpropagation. An alternative is to estimate the number of FLOPS (floating-point operations per

Table S6: Impact of batch size on SIESTA’s performance evaluated on ImageNet-1K without augmentation. The ( $\uparrow$ ) and ( $\downarrow$ ) indicate high and low values to reflect optimum performance respectively.  $\mu$  and  $\alpha$  denote average top-5 accuracy (%) and final top-5 accuracy (%), respectively. Total training time T is reported in hours.

Batch	T( $\downarrow$ )	$\mu$ ( $\uparrow$ )	$\alpha$ ( $\uparrow$ )
32	3.80	88.36	83.53
64	2.39	88.33	83.59
128	2.20	88.38	83.72
256	1.97	88.34	83.61
512	1.89	88.29	83.50

Table S7: Computational comparison among methods in terms of GFLOPS and total number of updates in million,  $\mathcal{U}$ . This is based on ImageNet-1K dataset. The ( $\uparrow$ ) and ( $\downarrow$ ) indicate high and low values to reflect optimum performance respectively.

Method	GFLOPS ( $\uparrow$ )	$\mathcal{U}$ ( $\downarrow$ )
DER	4021.61	12.43
REMIND	9188.17	11.53
<b>SIESTA</b>	<b>17393.40</b>	11.53

second) for each method. Here we estimate the number of FLOPS for a subset of the methods and juxtapose that with updates. FLOPS may be a more meaningful metric for SIESTA, since each update during sleep is only updating the  $\mathcal{F}$  and  $\mathcal{H}$  rather than all layers of the DNN; however, SIESTA does require compute for reconstruction that the other methods omit. The three models use the configurations for augmentation-free on ImageNet. GFLOPS were estimated with DeepSpeed<sup>1</sup> using the same hardware across methods (NVIDIA GeForce GTX TITAN X GPU).

GFLOPS for SIESTA, REMIND, and DER are given in Table S7 along with the total number of updates. SIESTA yields  $1.9\times$  higher GFLOPS than REMIND and  $4.3\times$  higher GFLOPS than DER. Thus SIESTA offers higher efficiency and throughput than compared methods.

In real-world continual learning, we could potentially have an infinitely long (never ending) data stream, which would be larger than ImageNet-1K, raising the question: how well do these models computationally scale to larger datasets? To find this, we measured the total computational costs associated with using a larger dataset by increasing batches where one batch corresponds to 100 classes from ImageNet-1K. Fig. S3 illustrates the computational comparison in larger scale beyond ImageNet-1K. It is evident that as size of dataset grows, the gap in GFLOPS between SIESTA and compared methods grows significantly. Thus

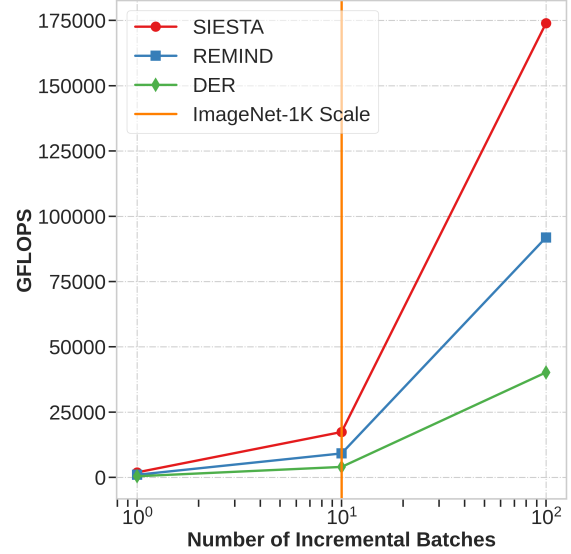


Figure S3: Comparison among methods based on GFLOPS. Each incremental batch corresponds to 100 classes from ImageNet-1K. This analysis does not apply any augmentations.

SIESTA becomes far more efficient than others in large scale regime.

<sup>1</sup><https://github.com/microsoft/DeepSpeed>